

AD_____

Award Number: W81XWH-FF

TITLE: V@^• @ |ãË, ã&@è^Áúæð^•Á\UÚ, Dú Â[} d[|Á\c^} æP^ { [|| @è^

PRINCIPAL INVESTIGATOR: Ö. E. A. [redacted]

CONTRACTING ORGANIZATION: University of Qā [ā
ÁMàæ æŠM Fì €Á

REPORT DATE: 06/01/2025

TYPE OF REPORT: Annual

PREPARED FOR: U.S. Army Medical Research and Materiel Command
Fort Detrick, Maryland 21702-5012

DISTRIBUTION STATEMENT: Approved for public release; distribution unlimited

The views, opinions and/or findings contained in this report are those of the author(s) and should not be construed as an official Department of the Army position, policy or decision unless so designated by other documentation.

REPORT DOCUMENTATION PAGE				Form Approved OMB No. 0704-0188	
Public reporting burden for this collection of information is estimated to average 1 hour per response, including the time for reviewing instructions, searching existing data sources, gathering and maintaining the data needed, and completing and reviewing this collection of information. Send comments regarding this burden estimate or any other aspect of this collection of information, including suggestions for reducing this burden to Department of Defense, Washington Headquarters Services, Directorate for Information Operations and Reports (0704-0188), 1215 Jefferson Davis Highway, Suite 1204, Arlington, VA 22202-4302. Respondents should be aware that notwithstanding any other provision of law, no person shall be subject to any penalty for failing to comply with a collection of information if it does not display a currently valid OMB control number. PLEASE DO NOT RETURN YOUR FORM TO THE ABOVE ADDRESS.					
1. REPORT DATE (DD-MM-YYYY) 01-12-2011		2. REPORT TYPE Annual		3. DATES COVERED (From - To) 23 Nov 2010 - 22 Nov 2011	
4. TITLE AND SUBTITLE Threshold-Switchable Particles (TSP's) to Control Internal Hemorrhage				5a. CONTRACT NUMBER	
				5b. GRANT NUMBER W81XWH-11-2-0021	
				5c. PROGRAM ELEMENT NUMBER	
6. AUTHOR(S) Dr. James Morrissey E-Mail: jhmmorris@illinois.edu				5d. PROJECT NUMBER	
				5e. TASK NUMBER	
				5f. WORK UNIT NUMBER	
7. PERFORMING ORGANIZATION NAME(S) AND ADDRESS(ES) University of Illinois Urbana, IL 61801				8. PERFORMING ORGANIZATION REPORT NUMBER	
9. SPONSORING / MONITORING AGENCY NAME(S) AND ADDRESS(ES) U.S. Army Medical Research and Materiel Command Fort Detrick, Maryland 21702-5012				10. SPONSOR/MONITOR'S ACRONYM(S)	
				11. SPONSOR/MONITOR'S REPORT NUMBER(S)	
12. DISTRIBUTION / AVAILABILITY STATEMENT Approved for Public Release; Distribution Unlimited					
13. SUPPLEMENTARY NOTES					
14. ABSTRACT The final goal of this project is to develop smart particles to stop internal hemorrhage at local sites. Four collaborating laboratories have worked together to define threshold levels of activators of blood clotting such that the candidate clotting activators will circulate in the blood at below the threshold necessary to trigger clotting, but accumulation of the activators at sites of internal injury/bleeding will cause the local concentration of clotting activators to exceed the clotting threshold and restore hemostasis. During the past year we have developed improved methods for attaching inorganic polyphosphate (a potent initiator and accelerator of blood clotting) to nanoscale solid supports, developed and tested several candidate procoagulant nanoparticles with adjustable abilities to trigger and/or accelerate blood clotting, addressed issues of biocompatibility of the nanoparticles, and made progress in defining the threshold levels under which these particles will or will not trigger blood clotting.					
15. SUBJECT TERMS Internal hemorrhage, Bleeding, Blood clotting, Nanoparticles, Trauma					
16. SECURITY CLASSIFICATION OF:			17. LIMITATION OF ABSTRACT UU	18. NUMBER OF PAGES 25	19a. NAME OF RESPONSIBLE PERSON USAMRMC
a. REPORT U	b. ABSTRACT U	c. THIS PAGE U			19b. TELEPHONE NUMBER (include area code)

Table of Contents

	<u>Page</u>
Introduction.....	1
Body.....	1
Key Research Accomplishments.....	13
Reportable Outcomes.....	13
Conclusion.....	13
References.....	15
Appendix (Supporting Data).....	17

FIRST ANNUAL REPORT: WQ81XWH-11-2-0021: "Threshold-Switchable Particles (TSP) to Control Internal Hemorrhage"

INTRODUCTION

The final goal of our research is to develop smart particles to stop internal hemorrhage at local sites. To accomplish this goal, we are combining multiple approaches in four collaborating laboratories to define threshold levels of activators of blood clotting such that the candidate clotting activators will circulate in the blood at below the threshold necessary to trigger clotting, but accumulation of the activators at sites of internal injury/bleeding will cause the local concentration of clotting activators to exceed the clotting threshold and restore hemostasis. The approaches being used include the development of novel chemistries for attaching inorganic polyphosphate (polyP; a potent trigger and accelerator of blood clotting) to nanoscale solid supports, development of candidate nanoparticles with varying abilities to trigger and/or accelerate blood clotting, and defining the threshold levels under which these particles will or will not trigger blood clotting.

BODY

Comments on Administrative and Logistical Matters

Subcontracts — Four laboratories participate in this project, headed by Drs. James Morrissey (University of Illinois at Urbana-Champaign, Ying Liu (University of Illinois at Chicago), Rustem Ismagilov (originally at the University of Chicago; now at Caltech), and Galen Stucky (University of California at Santa Barbara). The primary contract was awarded to the University of Illinois, with Dr. Morrissey as the PI. The Morrissey and Liu laboratories are at University of Illinois campuses (Urbana-Champaign and Chicago), so subaward contracts were not needed and grant accounts were set up for both investigators during the first quarter. The laboratories of Drs. Ismagilov and Stucky are located at other universities, which required negotiating subcontracts to both of these sites. The subaward agreement to the University of Chicago (Ismagilov lab) was completed in February 2011, so the Ismagilov lab initiated their studies near the end of the first quarter. The subaward agreement with the University of California at Santa Barbara (Stucky lab) was completed in March 2011, so the Stucky lab initiated their studies during the second quarter. Dr. Ismagilov moved his laboratory to Caltech in October 2011, and we are in the process of negotiating a new subaward contract to Caltech in order for Dr. Ismagilov to continue his studies funded in this project.

Human Anatomical Substances use approval (Milestone #2) — Some of the studies to be conducted in Dr. Ismagilov's lab will employ blood samples from human volunteer blood donors, which requires regulatory approval. Dr. Ismagilov has obtained IRB approval from Caltech for these studies (approved on December 5, 2011) and this was communicated on Thursday, December 8, 2011 to Ms. Brigit Ciccarello (Regulatory Compliance Specialist, Telemedicine & Advanced Technology Research Center, U.S. Army Medical Research and Materiel Command, Fort Detrick, Maryland), who submitted the necessary documents to obtain approval from the Office of Research Protections. No studies with human blood donors will be initiated until full approval is secured.

Scientific Progress

A. Detailed Simulations (toward Task 1, Milestone 1)

Dr. Ismagilov's lab began in the first quarter running simulations to test at what points the coagulation cascade is most susceptible to initiation. These simulations used a previously reported model that describes enzyme kinetics and stoichiometric inhibition in blood coagulation with 42 differential rate equations for 45 interacting species. For these preliminary tests, only kinetics were of interest and diffusion and fluid flow were not included. For activation of individual factors, preliminary results indicated that coagulation is initiated only if particular enzymes are activated: Factors XIIa, XIa, Xa, IXa, or IIa (thrombin). Activation of other individual enzymes such as plasma kallikrein, factors VIIIa, or Va do not lead to initiation of coagulation. In the second quarter, the Ismagilov lab

investigated the threshold concentration of each of these factors that was required to initiate clotting in the simulation. Intrinsic pathway factors IXa and XIa required only 10 pM concentrations, whereas downstream pathway factors thrombin and XI required 100 pM. The Ismagilov group also tested whether activating multiple factors is more efficient than activating single factors, and found that the clotting is accelerated up to four-fold by activating pairs of factors. Consistent with previous results, the fastest combinations included thrombin and either factor XIa or IXa. No further acceleration was obtained by activating three factors at once, which tells us that prototype nanoparticles need produce, aggregate, or accumulate only one or two activated factors in order to have a strong effect. These results contribute to progress towards Milestone 1 (Identifying conditions that result in thresholds for initiation of coagulation).

In the third quarter, Dr. Ismagilov's lab began testing the effects of spatially clustering patches of activators by using numerical simulations of blood clotting. They conducted simulations of spatially patterned clusters of particles that activated two factors (thrombin and factor X) to determine whether clustering or confinement of such particles was sufficient to initiate clotting. Whereas a dilute suspension of particles did not initiate clotting, particles clustered 500-fold or more did initiate clotting, by raising the local concentration of downstream clotting factors such as Xa and allowing the system to cross the threshold for coagulation. Particles clustered only 50-fold did not initiate clotting. This result suggests that particles that activate a pair of factors at a constant but low rate can initiate clotting if they are targeted to the site of hemorrhage and accumulate there at high concentration, while small aggregates that form by chance elsewhere in the bloodstream are safe and will not induce undesired clotting. These results again contribute to progress towards Milestone 1 (Identifying conditions that result in thresholds for initiation of coagulation).

Dr. Ismagilov's lab moved from the University of Chicago to Caltech during the fourth quarter. Dr. Shencheng Ge, a postdoc working on the project, continued to investigate proposed mechanisms for TSP-induced blood coagulation using numerical simulations (Milestone 1). The group also obtained Caltech IRB approval and approval from the Institutional Biosafety Committee for work with human blood samples (progress toward Milestone 2). However, since the subaward with Caltech has not been approved yet, the group did not receive funding since the move and work on microfluidic tests of clotting (a move towards Milestone 3) could not continue. The group anticipates beginning work towards Milestone 3 once the subaward contract to Caltech is completed, initially using commercially-available pooled human plasma until the human subjects use is approved by the DoD.

B. Particle Design and Tests – Morrissey and Liu Labs (toward Tasks 3a and 3b, Milestone 4)

The Morrissey and Liu labs have collaborated closely to conjugate polyP onto the surfaces of organic and inorganic particles to investigate the effects of particle surface properties (i.e. surface charges and ligands) and particle sizes. An important next step is to generate hybrid particles with thermal sensitive or chemically responding polymers and polyP at the surface. Under the switch conditions (such as, lower temperature or over expressed chemicals), the polymer brushes are extended or folded to either shield or expose the surface ligands such as polyP.

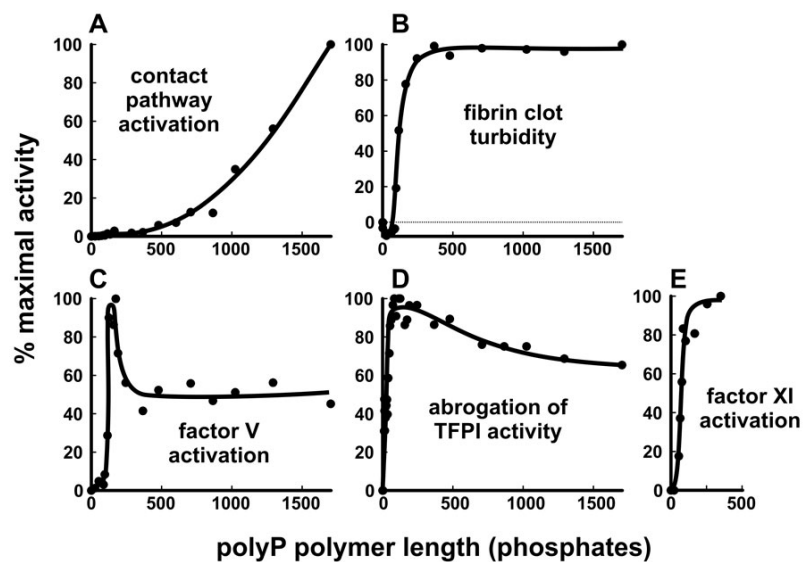


Figure 1. Size-dependence of polyP's procoagulant activities. Data are replotted as % maximal activities versus polyP polymer length from Smith et al. [1] and Choi et al. [2].

In 2006 the Morrissey lab discovered that polyP, which is secreted by activated platelets and which accumulates in infectious microorganisms, activates and accelerates the clotting cascade [3]. Subsequent studies from the Morrissey lab have further delineated the steps in clotting that are enhanced by polyP [1, 2, 4-6]. In particular, detailed studies of the size dependence of polyP's procoagulant activities have shown that shorter polyP polymers (of the size secreted by platelets) are potent at accelerating the activation of factors V and XI, while much longer polyP polymers are required to initiate clotting via the contact pathway (see Figure 1). These findings allow us to tailor the specific procoagulant activity of polyP-containing nanoparticles by varying the polyP polymer lengths used, as well as by controlling the amount of polyP per particle. The engineered particles should therefore have the capacity to induce clotting in a controlled and directed manner, compared to free polyP.

The interaction between foreign particles and blood plasma could cause a series of events, including the adsorption of albumin, IgG and fibrinogen, platelet adhesion and activation, and thrombosis [7]. Previous results show that foreign particles could shorten the clotting time [8], depending on the concentration, size and surface properties of the particles [9]. Mechanisms of particle-blood plasma interactions have not been fully studied, so an important goal is to understand the how engineered particles modulate clotting, and to optimize their properties.

The Morrissey lab recently reported a novel method for covalently attaching polyP to primary amines [10], which greatly facilitates polyP-nanoparticle assembly. This reaction uses the zero-length cross-linking reagent, EDAC (1-ethyl-3-[3-(dimethylamino)propyl]carbodiimide), to promote the formation of stable phosphoramidate linkages between primary amines and the terminal phosphates of polyP. However, the efficiency of the polyP labeling reaction is not efficient and furthermore, the reaction as reported requires the organic molecule (or particle) contain primary amines. Under this project, the Morrissey lab has worked to enhance the reaction conditions and also to modify the method to introduce other functional groups onto the termini of polyP, in order to broaden the types of coupling reactions it could participate in. Accordingly, we have found that we can achieve nearly 80% end labeling using polyamines such as spermine and spermidine. Furthermore, the reaction product now contains primary amines attached to the ends of the polyP polymers, which can now be reacted with a wide variety of derivatizing reagents that target primary amines. We are also working on introducing free sulfhydryl groups onto the termini of the labeled polyP polymers, in order to use sulfhydryl-labeling chemistries. These findings are allowing additional types of chemistries to be used to couple polyP to particles.

The Liu lab has modified or chose particles with multiple terminal amine surface groups and collaborated with the Morrissey lab to conjugate a controlled number of polyP with these surface amines. Work from the Morrissey lab indicated that PAMAM dendrimers associate tightly with polyP and might therefore serve as a platform for assembling polyP-containing nanoparticles. PolyP conjugation to three types of particles (G4Poly(amido amine) (PAMAM) dendrimers, amino polystyrene, and amine ligands bound to gold nanoparticles) were investigated in Liu lab to verify three hypothesis: (1) plasma clotting kinetics and mechanism would be affected by the size (or curvature) of the particles and an optimized condition could be selected; (2) the choice of the biocompatible core material would not change the plasma clotting kinetics or mechanism; and (3) the functionalities of the particles would be determined by the surface properties (i.e. neutral vs. charges and the chain length of polyPs) (work toward Milestones 3 and 4).

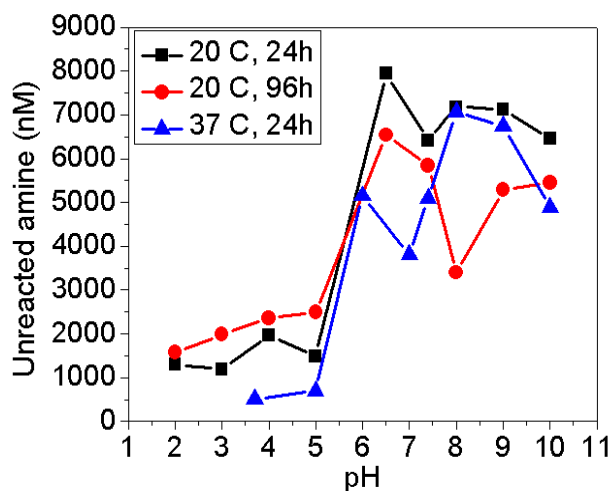


Figure 2. The efficiency of dendrimer-polyP conjugation at different pH, temperature and time conditions.

In the near future, we will measure how the total number of polyP chains affects clotting of plasma, and compare whether the mechanism and time to clot changes with free chains of polyP. Three control groups were selected to compare with the particles-polyP conjugates: (1) free polyP with the same molecular weight at the same concentration; (2) linear polyP with the molecular weight equivalent to the summation of polyP the molecular weight attached on a single particle (i.e. polyP molecular weight times the conjugation number); and (3) particles without polyP.

Dendrimer-polyP conjugation

PolyP (45-mer) was conjugated to the G4 PAMAM dendrimer, which has 64 primary amines on the surface. The zero-length cross linking reagent, EDAC was used to couple primary amines to phosphates via phosphoramidate linkages [10]. The separation of free polyP and dendrimer-polyP conjugate was done by employing size exclusive columns. The plasma clotting efficiency was tested by using a viscosity based coagulometer.

To find out the optimized conditions for conjugation, various conditions, such as the temperature, pH and reaction time were tested. The fluorescamine assay was used to test the amount of the unreacted primary amines on dendrimer, which indicated us the conjugation efficiency

The conjugation efficiency under various conditions were tested and shown in Figure 2. The reactions were more efficient at low pH conditions. The amine concentration before the reaction was about 3400 nM. Some of the data shows even higher amine concentration after reaction compared to the control was due to the degradation of the dendrimer (discussed below). The optimized condition was selected as 4 hours at 37 °C and pH 4, after which >80% of the primary amine on dendrimer had reacted with polyP.

Dendrimer and polyP Stability

The stability of polyP at 37 °C after 24 hours was tested as a function of pH (Figure 3). Compared to the sample at pH 7.4, there was no increase of free phosphate, which indicated little degradation. Therefore, polyP was stable

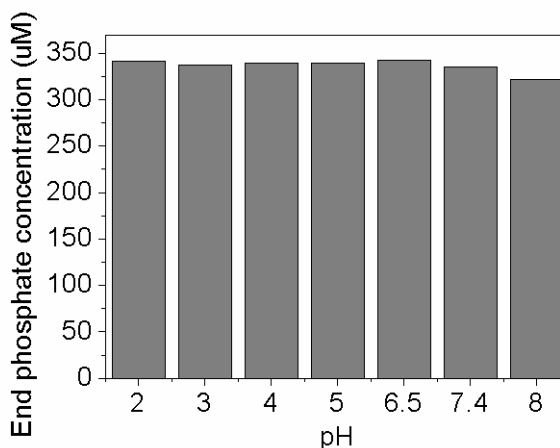


Figure 3. Stability of polyP at 37 °C and various pH conditions.

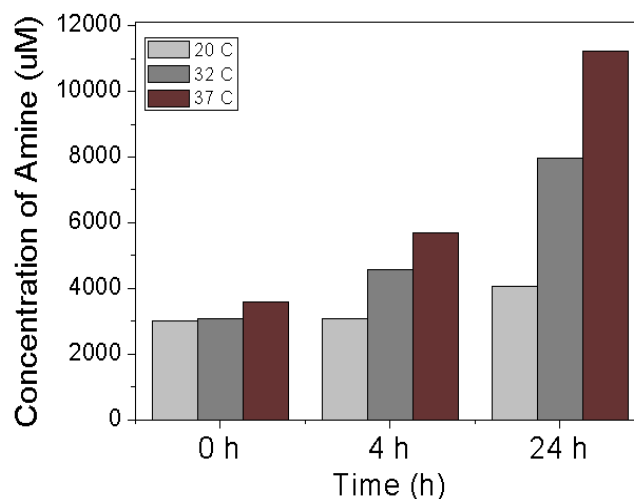


Figure 4. Stability of dendrimer at various conditions.

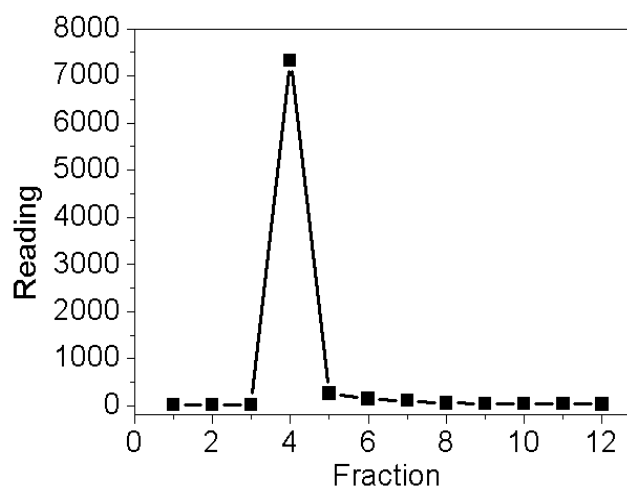


Figure 5. Dendrimer running through the Econo-Pac 10 DG Columns. The running phase was DI water.

for the first 24 hours at 37 °C and as low as pH 2.

The stability of dendrimer at various conditions was also tested. Below pH 4 and above 32 °C, more than 25% dendrimer degraded within 4 hours. At 20 °C and pH 4, the dendrimer was stable for the first 4 hours and about 10% degradation happened at 24 hours.

Separation

Econo-Pac 10DG Columns were first used to separate the free polyP and dendrimer-polyP conjugates. Recovery of dendrimer was highly depend on the running phase. When purified water was used as the running phase, as shown in Figure 5, the dendrimer eluted in the 9th fraction but recovery of dendrimer was only about 5%. We hypothesized that most of the dendrimer was trapped in the column because of ionic interactions. Therefore, in later experiments, buffers with at least 20 mM salt concentration were used to eliminate the effect of ionic interactions between the gel and the solute. As an example, with 25 mM borate acid buffer at pH 9, dendrimer eluted at the 4th fraction and recovery rate was above 85% (Figure 6). Dendrimer-polyP conjugate was then separate on the column (Figures 7 and 8). The dendrimers eluted at the 6th fraction, while the peak of polyP was from the 5th fraction to the 7th fraction. Therefore, separation of free polyP from the conjugate through the Econo-Pac 10 DG Column was not achieved.

Size exclusion columns packed with Bio-Gel® P-10 gel were then used for the separation of conjugated polyP from the un-reacted polyP. Bio-Gel® P-10 Gel with a molecular weight (MW) fractionation range from 1,500-20,000 was selected, which should be suitable to separate the polyP-dendrimer conjugation (MW>20,000) from the un-reacted ones (MW<13,700) The dendrimer eluted at the 10th fraction and the polyP came out at the 9th fraction (Figures 9 and 10), which was deemed insufficient separation.

Another separation method tested was with “glass milk”, which consists of silica particles in aqueous solution. The glass milk used for experiments in the Liu lab was obtained from the Morrissey lab. 1 µL of glass milk is added to 500 µL of dendrimer-polyP reaction. The glass milk and reaction was then mixed for 30 minutes with occasional vortexing. After mixing, the solution was then centrifuged for 10 minutes at 3,500 RPM. The purified supernatant was collected and the malachite green assay (which quantifies phosphate following acid digestion of polyP) was performed to quantify polyP concentration against the same reaction that had not undergone glass milk purification. Figure 11 shows a decrease in phosphate concentration of over 90% before and after the glass milk separation.

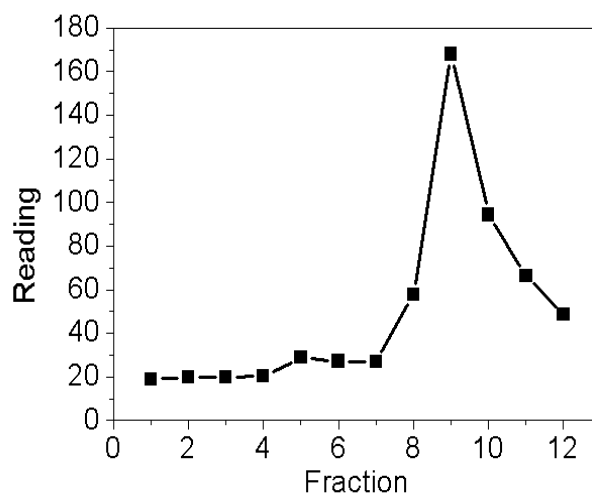


Figure 6. Dendrimer running through the Econo-Pac 10 DG Columns. The running phase was 25 mM borate acid buffer at pH 9.

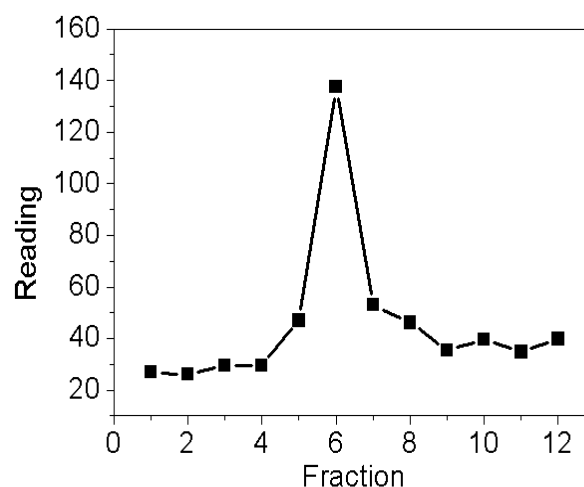


Figure 7. Dendrimer-polyP running through the Econo-Pac 10 DG Columns. The running phase was borate acid buffer. The reading was for dendrimer.

After these initial results, the glass milk assay was performed again and both the malachite green and fluorescamine assays were performed to ensure that only free polyP was removed by the glass milk and that the dendrimer remained in solution. The results in figure 12 indicated less efficient separation of polyP than the previous experiment as well as a similar decrease in primary amine and polyP concentrations before and after the glass milk assay. We also found in these results that the concentration of primary amine in the control reaction had increased from the initial amount expected before reaction. This lead us to believe that the reacted dendrimer was degrading over time.

Clotting tests

Plasma clotting times were tested by using a coagulometer. The sample was dendrimer-polyP conjugate which reacted at 37 °C, pH 4 for 24 hours. The clotting time for this sample was 143.8 seconds.

Polystyrene (PS)-polyP conjugation

General procedure for making the PS-polyP conjugation:

- 1-2 mL reactions were setup using conditions previously described in amine polyP reactions [10].
- 250 mM of 45-mer polyP was added from an aqueous bulk solution made from sodium phosphate glass purchased from Sigma Aldrich.
- 100 mM pH 4 MES buffer was added to the reaction.
- 300 mM of EDAC was added to the reaction to activate the reaction between polyP and primary amine.
- The amount of primary amine on the surface of the PS particle was characterized using fluorescamine assay. 0.21 mM of primary amine was added to the solution. This is approximately 5 times less than the concentration of polyP chains.
- The reaction was brought up to volume with DI water.
- The reaction was allowed to proceed for up to 24 hours with vigorous stirring with the concentrations of primary amine consumed tested at various time points.

Polystyrene beads (diameter of 50 nm) with primary amine as the surface functional group were used to conjugate polyP. The optimized reaction condition was 20 °C and pH 4. After 24 hours, more than 60% of the primary amine was reacted with polyP (Figure 14).

The stability of PS beads was tested. As shown in Figure 15, the amount of amine was stable at 20 °C, but increased at 37 °C. The hypothesis was that at higher temperature and low pH, amine groups buried inside the particles could be exposed on the surface. Therefore, the reaction efficiency was underestimated.

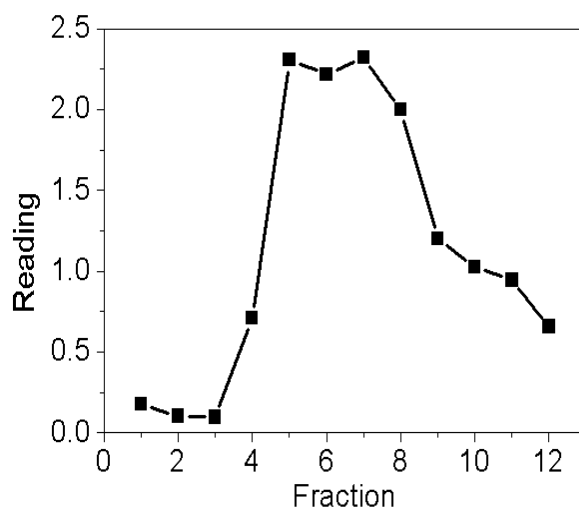


Figure 8. Dendrimer-polyP running through the Econo-Pac 10 DG Columns. The running phase was borate acid buffer. The reading was for polyP.

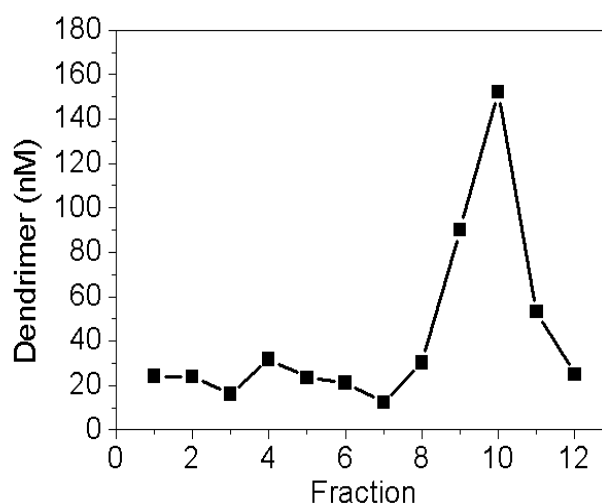


Figure 9. Dendrimer-polyP running through the BG P-10 Gel packed columns. The running phase was 1M LiCl. The reading was for dendrimer.

Gold nanoparticle-polyP conjugation

General Reaction Mechanism:

A. A bulk solution of the thiol-amine ligands of 10.2 mM was made in water and stored at 4°C.

B. PolyP and amine ligands were reacted as previously described with a ratio of 5:1 excess of polyP. Reactions were performed in pH 4 MES Buffer at 37°C and at ambient temperature (25°C).

C. The amount of reacted ligand was determined using the fluorescamine assay.

D. Thiol-reacted ligands were bound to 5 nm citrate-coated gold nanoparticles [11] by adding a 20x dilution of the ligand reaction with an excess of 50:1 thiol ligand to gold nanoparticles. We predicted that there will be between 12-16 ligands bound to each nanoparticle based on previous studies that found that 130 ligands were normally bind to 15nm gold nanoparticles [11].

E. The mixture was periodically vortexed and continuously mixed for 8 hours.

F. The gold nanoparticle mixture was centrifuged at 13,500 RPM for 20 minutes to remove excess polyP and unbound ligands.

G. The supernatant was removed and the pellet was washed and resuspended with 450 μ L DI water.

H. The centrifuging and washing was repeated twice.

I. UV spectroscopy, malachite green assays, and fluorescamine assays were performed to quantify the number of polyP chains bound the surface of the gold nanoparticle.

A preliminary study of the reaction of amine ligands with polyP at 37°C

demonstrated that primary amine levels decreased around 75% after 24 hours of reaction, indicating a 75% reaction completion of amine with polyP. However, the level of primary amine increased to approximately half of its control concentration after 48 hours which suggests that bonds may have hydrolyzed. The concentration of amine in the control at 37°C essentially did not change suggesting that the difference in the reaction amine concentration cannot be explained by the assay itself.

The thiol-amine ligand reaction at with polyp at room temperature was shown to have been completed between 75% to 80% of the ligands in solution. Figure 18 details the results of the reaction optimization. The concentrations in the above reaction scheme except with a 0.42 mM concentration of amine bound ligand, yielded approximately a 5:1 ratio of polyP chains to amine. Comparing the reactions performed at 37°C with the ones performed at room temperature, we found further indication that the bonds of the amine-polyP did indeed hydrolyze at 37°C over time. Therefore, we concluded that both reactions had similar efficiencies and after 72 hours at room temperature more than 75% amine was consumed.

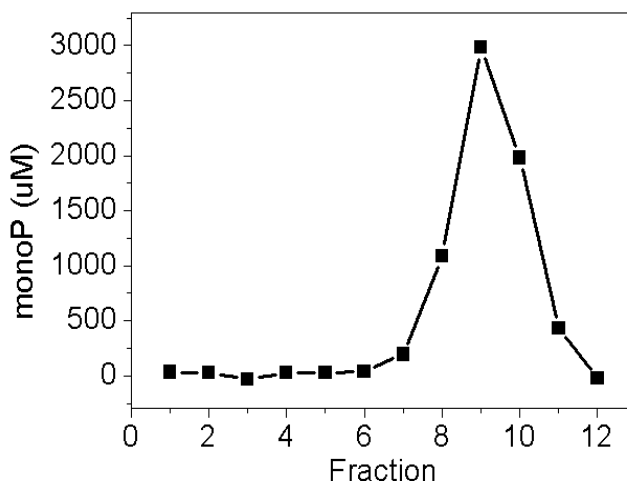


Figure 10. Dendrimer-polyP running through the BG P-10 Gel packed columns. The running phase was 1M LiCl. The reading was for PolyP.

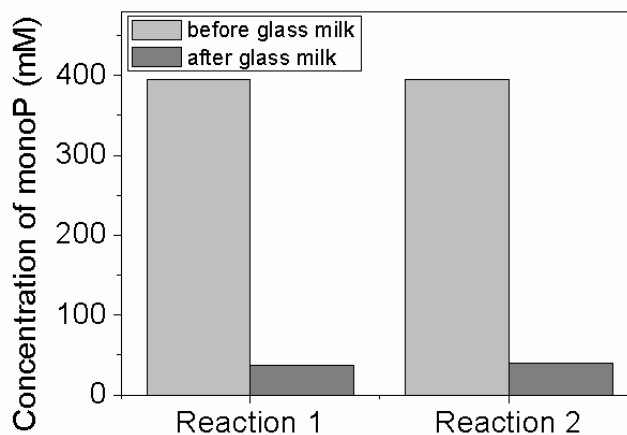


Figure 11. PolyP concentration before and after glass milk assay performed on two previous reactions.

Different ratios of polyP to amine were tested, which should affect the final ratios of amine-thiol ligand to the polyP-thiol ligand. The completed reactions mixed with gold nanoparticles were able to be successfully pelleted after centrifugation (Figure 19).

In the future, the Liu lab will mainly focus on the modification of gold nanoparticles, because of the following advantages: (1) easy to produce at various particle sizes; (2) conveniently to modify with the well-studied reaction mechanisms; and (3) easily to separate or purify. However, to demonstrate that the core material would not affect the clotting kinetics, we will (1) compare the gold-polyP conjugates with other particles, and (2) crosslink a thin polymer layer and then dissolve the gold. The following studies are planned:

- Reaction condition will be optimized to maximum the gold-polyP conjugation. The primary amines on the surface of gold nanoparticles react with polyP through phosphoramidate linkages, by employing the zero-length cross-linking reagent, EDAC. Based on our previous experiments, the conjugation efficiency depends on various conditions such as pH, temperature and time. Meanwhile, polyP and the phosphoramidate linkages also some undergo hydrolysis at low pH and high temperature conditions. Therefore, the optimized conditions need to be found to ensure the samples have high conjugation efficiency and low hydrolysis rate.

- The optimized conditions for the separation process will also be studied. Centrifugation will be used to separate gold-polyP conjugation and unreacted polyP. Our previous result shows that gold nanoparticles could be successfully pelleted during centrifugation. The concentration of gold and polyP in the supernatant and pellet will be test by using UV-vis spectroscopy and malachite green assay.

- The plasma clotting efficiency of the gold-polyP conjugation will be tested in vitro and in vivo by using a coagulometer and microfluidic devices.

- Gold nanoparticles with different sizes and polyP with different molecular weights will be used for the conjugation to test the effects of surface curvature and surface density of polyP on the plasma clotting efficiency. Moreover, blended ligands (neutral and charged) will be conjugated on the surface of the gold particle together with polyP. The change of nanoparticle sizes will result in different surface curvature, conjugation number and surface density of polyP. PolyP with different MW, such as 45mer, 70mer and >200mer, will be used.

- Thermo-sensitive polymer (longer than polyP) will be co-attached on the gold particles. The folding and unfolding of the polymer will be tested. The plasma clotting kinetics at switchable conditions with the particles with hybrid ligands will be tested.

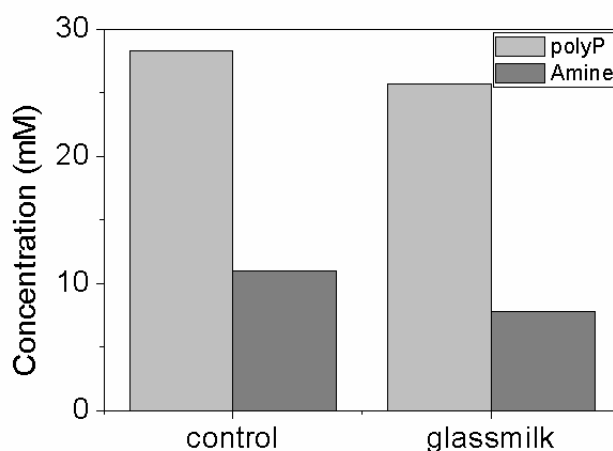


Figure 12. Concentration of primary amine and PolyP before and after glass milk separation assay.

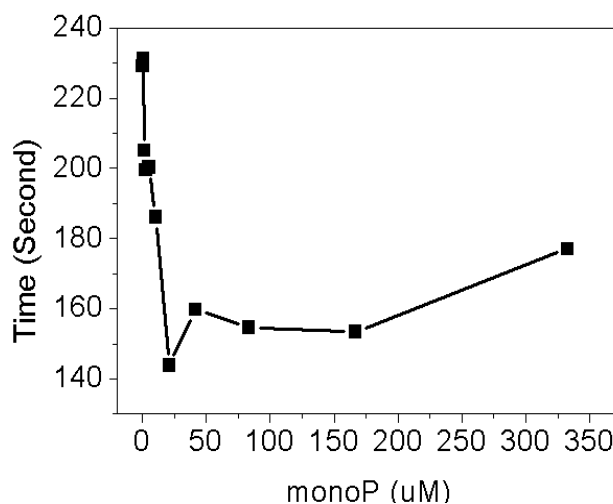


Figure 13. Blood clotting test for Dendrimer-PolyP conjugation.

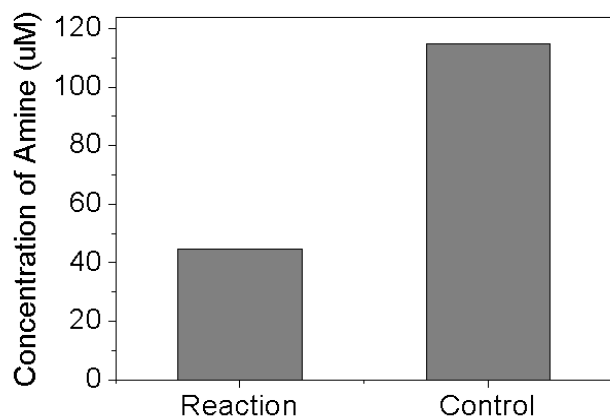


Figure 14. PS-polyP conjugation. The reaction conditions was at room temperature, pH4, and 24 hours.

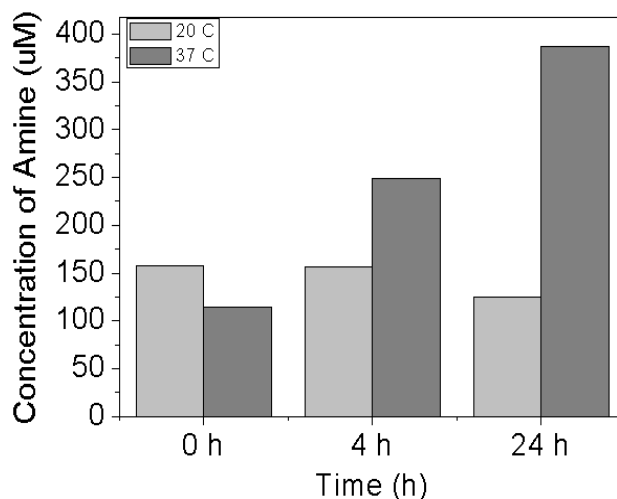


Figure 15. The amount of amine exposed on the surface of the PS particles at pH 4.

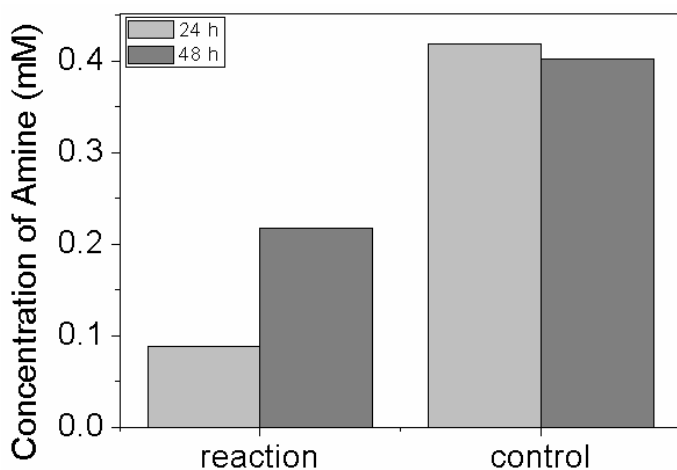


Figure 16. 24 and 48 hour primary amine concentration of a ligand polyP reaction vs. control under the same conditions except without EDAC.

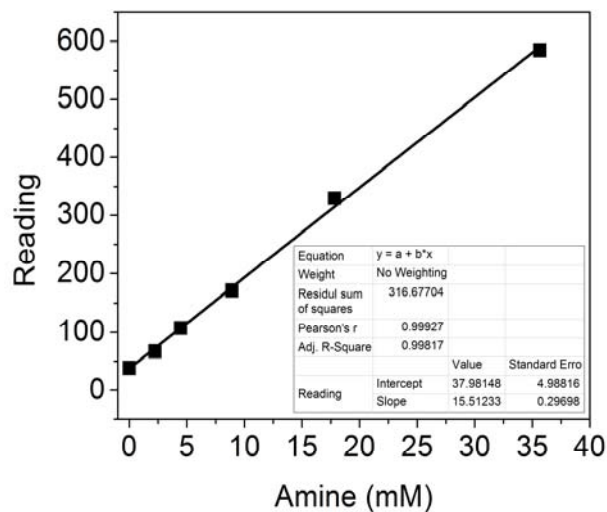


Figure 17. Calibration curve of primary amine concentration at excitation and emission wavelengths of 410 and 480 nm respectively.

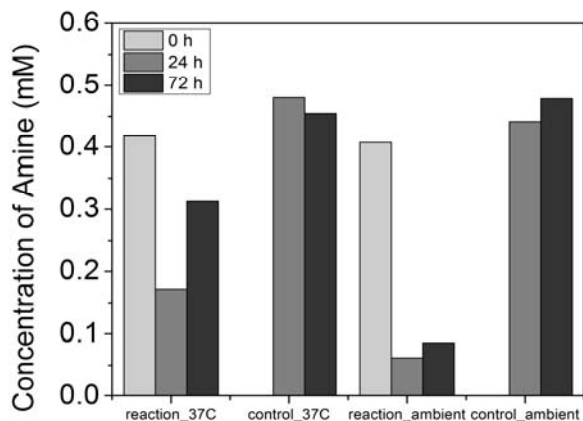


Figure 18. Primary amine concentration after the amine-thiol ligand reacted with polyP.

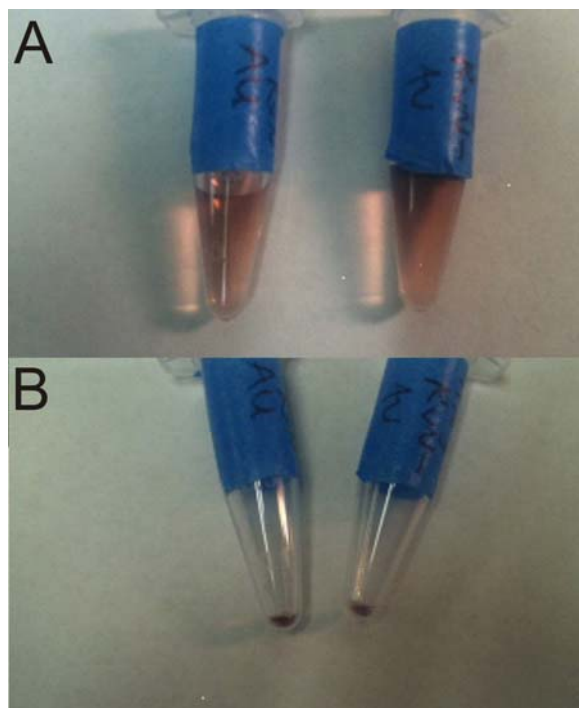


Figure 19. A. The gold nanoparticles ligand mixture before centrifugation. B. Gold particle pellet after centrifugation.

C. Particle Design and Tests – Sticky Lab (toward Tasks 3a and 3b, Milestone 4)

Work at UCSB has focused on designing and synthesizing new and recently developed solid and porous nanoparticle materials that exhibit biocompatibility and rapid thrombus formation. More importantly, the nanoparticles must restrict activity to a local region of above-threshold coagulation activity. Research into specific nanoparticles focuses on two particles – procoagulant silica and medical implant compatible titania [12]. The nanoparticle scaffolds are functionalized with a procoagulant compound – thrombin, tissue factor, or polyP – to form a threshold-switchable particle (TSP) that further promotes clot formation. Thrombin, the key protein in the coagulation cascade, has a hydrodynamic radius of roughly 8.4 nm [13]. A porous nanoparticle must have a minimum pore size of 10 nm to load thrombin. Characterization of the particles includes microscopy, zeta potential, dynamic light scattering, and other tests. Thromboelastography (TEG) plasma clotting experiments studied the procoagulant activity of naked and functionalized nanoparticles introduced to recalcified pooled normal plasma (PNP).

Silica Nanoparticle Synthesis – Task 3.a (toward Milestone 4)

Our silica synthesis seeks to create a porous nanoparticle with a diameter smaller than 200 nm and a pore size greater than 20 nm. This particle will have the minimum size necessary to avoid organ damage, while able to transport and deliver thrombin and other coagulation factors. A porous particle with these specifications has not previously been reported.

Initial nanoparticle syntheses began with attempts to synthesize mesoporous mesocellular foam with a 26 nm pore size (MCF-26) and particle diameter below 1 μm . Mesocellular foams (MCF) with pore sizes of 11.2 nm, 24.3 nm, and 30.9 nm pore size were created. The foams were all characterized using BET. Window size was determined from desorption isotherms using the Broekhoff- de Boer (BdB) method; pore size from the adsorption isotherm using the same BdB method [14]. Particle diameters were measured using scanning electron microscopy (SEM) imaging.

The ability to precisely define pore sizes in the range desired for enzyme and large biomolecule delivery has been clearly demonstrated. The experimental reconciliation of this pore size creation capability with the smallest possible particle size (< 200 nm) desired for cardiovascular delivery is still being developed using the MCF and the alternative approaches described below.

A second new synthesis procedure (unpublished) was developed for the synthesis of flocculated mesoporous silica (FMS) particles with nanofiber or nanosphere morphology (FMS-nf, FMS-ns).¹ FMS-nf and FMS-ns were chosen in an attempt to synthesize nanoparticles under 200 nm. Dynamic light scattering indicated a particle size of 250 +/- 50 nm. This is a step in the right direction and is being further pursued. Many of the capping and coagulation experiments were carried out using FMS silica nanoparticles.

These two procedures entail the use of solution sol gel or colloidal silica precursors. This suggested that the lessons learned from the synthesis and processing of biocompatible polymers for small molecule drug delivery might be applicable for the synthesis of the desired large pore, nanoparticle enzyme delivery agents. Our new silica synthesis methodology based on the previously established poly(lactic-co-glycolic acid) (PLGA) method for drug delivery is shown in Figure A-4 in the Supporting Data below [15]. The silica synthesis procedure uses trimethylbenzene (TMB) and NH₄F [16, 17] used in the MCF synthesis; and a triblock copolymer, P123, combined with a cationic surfactant, CTAB [18], to create a liquid silica precursor. Using this approach, we successfully synthesized silica particles with average nanoparticle diameters of 125 +/- 25 nm. The 18.2 nm pore size is sufficient for embedding thrombin. This is within the desired range of our large pore, nanoparticle synthesis goal. Work will continue using the PLGA scheme to optimize the particle diameter and porosity with respect to thrombin delivery, the most efficient use of particles, and biocompatibility. Using the PLGA methodology, we have nearly achieved our goal of a small diameter mesoporous silica nanoparticle with sufficient pore size for protein transport and delivery.

Another tactic to restrict activity to a localized threshold region is to use solid silica and titania nanoparticles as carriers. We will work with the Ismagilov group to determine the threshold conditions for capped and uncapped solid nanoparticles [19]. In the coming year, the Stucky group aims to synthesize solid silica nanoparticles with particle diameters between 5 – 100 nm. Capping procedures will be used to bind polyP and coagulation factor proteins to the nanoparticle surface. The procedures will aim to synthesize solid silica nanoparticles with system residence times, polyP and thrombin loadings that are precisely defined to enable restriction of their activity to a local region of above-threshold coagulation activity.

Titania Nanoparticle Synthesis – Task 3.a (toward Milestone 4)

One concern about procoagulant silica compounds is that uncapped silica injected into the bloodstream may lead to general clotting [19]. Spontaneous general clotting would make nanoparticles unfit for internal hemorrhage treatment. Titania has been proven to be biocompatible [12]. In particular, anatase titania nanoparticles have been shown to exhibit anticoagulant properties, thus increasing clotting times and reducing clot strength [20]. Titania particles in the bloodstream will not cause clots in healthy bloodstreams. In the presence of vessel injury, the procoagulant molecules loaded to the scaffold will activate to accelerate coagulation.

Titania nanoparticles were synthesized via a phosphoric acid pathway and characterized using SEM and X-ray diffraction [21]. The particle diameters averaged 225 +/- 50 nm. Along with the silica FMS, titania particles were used in functionalization studies.

PolyP capping – Task 3.b (toward Milestone 4)

Stucky group research into polyP capping focused on two pathways. The first pathway utilized the Lewis acid properties of both silica and titania. Lorenz et al. successfully bound polyP to zirconia [22]. The process was adapted by replacing zirconia with either silica or titania. The negative shift in zeta potential illustrated in Figure A-3 in the Supporting Data below indicates polyP successfully bound to its target.

¹ In preparation for publication.

The second pathway uses (3-aminopropyl)-triethoxysilane (APTES) to form a bridge between the nanoparticle and the procoagulant material. The primary amine terminus of APTES readily binds with proteins or EDAC-modified polyP. The Morrissey group has shown how polyP binds to amine surface strip wells using EDAC, polyP, APTES-modified silica, and 2-(N-morpholino)ethanesulfonic acid (MES) [10]. Zeta potential and Fourier transform infrared (FTIR) spectroscopy showed that the nanoparticles had been functionalized with APTES. Zeta potential measurements were used to ensure that the polyP bound to the particles.

Protein Capping – Task 3.c (toward Milestone 4)

In collaboration with Dr. Gary Braun of the Dr. Erkki Ruoslahti group at UCSB, we developed a new procedure for capping solid nanoparticles with thrombin using the APTES mechanism described above. The mechanism involves binding a slowly deprotected thiol on the APTES-nanoparticle scaffold to the thiol-reactive group on the protein. In theory, this pathway will minimize aggregation of particles and proteins due to a fast reaction rate that would result in one particle binding to one protein. We will investigate this procedure to load solid silica with proteins such as thrombin in the first quarter of 2012.

In the future, other parts of the coagulation cascade will be integrated with the nanoparticles to determine efficacy in treating internal wounds. One nanoparticle carrier pathway involves initiating coagulation using a tissue factor (TF)-Nanodisc agent developed by the Morrissey group [23]. Other molecules such as fibrinogen are found in non-coagulating blood. During coagulation, thrombin converts fibrinogen into fibrin monomers. The monomers cross-link at the wound site to form fibrin polymers, which act as a backbone to form the clot [24]. Delivering additional fibrinogen to a wound site can replenish the fibrinogen concentration and perhaps lead to a stronger clot.

Thromboelastography – Task 3.d (toward Milestone 4)

Several silica samples – both naked and polyP capped – were tested for procoagulant activity using plasma in a thromboelastograph (TEG) instrument. The TEG measurement focused on four coagulant parameters: R, time until first clot; K, time from initial clot formation to 20 mm clot diameter; α , clot formation speed; MA, clot strength. As listed in Table 3, these data suggest that the polyP-capped silica decreased the time and speed of clot formation. However, the lower MA values suggest the silica also reduces the clot's strength. We will continue to investigate the coagulant activity of proposed TSPs in the coming year.

Biocompatibility – toward Milestone #8

Some concern exists over cytotoxicity levels of particles in the human body. The Stucky lab's collaboration with Dr. Daniele Zink of the Institute of Bioengineering and Nanotechnology, ASTAR, in Singapore, examines the cytotoxicity of MCF-26 on human cells.² Dr. Zink's group tested MCF-26 absorption by HUVEC (Human Umbilical Vein Endothelial Cells), HEK-a (Human Embryonic Kidney), HDF-a (Human Dermal Fibroblast), HPTC (Human Renal Proximal Tubule), HK-2 (Human Kidney 2), and NIH-3T3 fibroblast cells. The cytotoxicity studies show that MCF-26 NPs are not toxic, even at extremely high concentrations. Typically, silica particles have IC_{50} values in the $\mu\text{g/ml}$ concentration range. In contrast, even for the highly sensitive HUVEC cells, MCF-26 IC_{50} values ranged between 0.7 – 6.3 mg/ml. Cells did not readily absorb MCF-26 particles until the concentrations reached the mg/ml scale. These studies show that porous silica is safer to use in treating internal hemorrhage than coagulating agents such as kaolinite. Our collaboration will continue in the next year as we will test all our nanoparticles to insure biocompatibility.

² In conjunction with Dr. Zink's group, the Stucky group is currently drafting a manuscript on these results with the aim to publish in the new year.

KEY RESEARCH ACCOMPLISHMENTS

- Used simulations to identify points in coagulation cascade most susceptible to initiation (Task 1, Milestone 1)
- Simulations identified threshold concentrations of clotting factors required to initiate clotting (Task 1, Milestone 1)
- Discovered that clotting is stimulated up to 4-fold by activating pairs of clotting factors, with no further stimulation using three activating pairs of clotting factor (Task 1, Milestone 1)
- Progress in understanding effects of spatial clustering of clotting activators on initiation of clotting (Task 1, Milestone 1)
- Improved reaction conditions for covalent linkage of primary amines to polyP (Task 3b)
- Extended chemistries developed for derivatizing the ends of polyP molecules (Task 3b)
- Developed PAMAM dendrimer-based, polyP-containing procoagulant nanoparticles; tested stability and activity (Tasks 3a & 3b)
- Developed polyP-containing polystyrene procoagulant nanoparticles; tested stability and activity (Tasks 3a & 3b)
- Developed polyP-containing gold procoagulant nanoparticles; tested stability and activity (Tasks 3a & 3b)
- Synthesized 125 +/- 25 nm particle diameter and 18.2 nm pore size (Task 3.a)
- Established human cell biocompatibility of porous silica (Milestone #8)
- Developed new particle synthesis procedure for delivery of thrombin, which has a hydrodynamic radius of 8.4 nm (Task 3.b)
- Synthesized titania particles with 225 +/- 50 nm average diameter (Task 3.a)
- Attached polyP chains to silica and titania nanoparticles using Lewis acid-base chemistry and APTES-EDAC mechanism (Task 3.b)
- Developed large quantity synthesis for polyP-bound nanoparticles as illustrated in Task 3.b (Task 3.c)
- Quantified procoagulant activity of silica and polyP-bound silica (Task 3.d)

REPORTABLE OUTCOMES:

- Damien Kudela, PhD candidacy, July 28th, 2011
- Stucky GD, "Molecular assembly of material systems with integrated nanoscale to macroscale functionalities," The 2nd International Symposium on Advanced Composite Materials, Tokyo, Japan, November 7-8, 2011.
- Stucky GD, "Zeolites and R. M. Barrer Inspired Control of Bioprocesses: The Challenge of Hemostasis," The Pennsylvania State University Barrer Lecture, University Park, PA, April 14, 2011.
- Stucky GD, "Controlling Bioprocesses with Inorganic Nanostructured Systems: The Challenge of Hemostasis," University of California, Berkeley Student-Hosted Inorganic Chemistry Series, Berkeley, CA, February 25, 2011.

CONCLUSION

Specific Aim #1 of the statement of work calls for using theory and experiments to identify the most promising mechanisms to switch from below- to above-threshold conditions to initiate local clotting. We made progress in using simulations to identify points in the coagulation cascade that are most susceptible to initiation and in identifying threshold concentrations of clotting factors required to initiate clotting. A new finding in these studies was the discovery that clotting is stimulated up to 4-fold by activating pairs of clotting factors, with no further stimulation seen by using three activating pairs of

clotting factor. In addition, further progress was made in understanding the effects of spatial clustering of clotting activators on initiation of clotting.

Specific Aim #2 of the statement of work calls for the design of a threshold-switchable particle system with a paired particle and trigger to target internal hemorrhage. The proposal calls for us to identify nanoparticles as scaffolds and to test procedures for attaching procoagulant materials to the nanoparticles. The Morrissey lab has further refined the chemistry for covalently attaching polyP to particles and amine-containing organic compounds as the basis for nanoparticle formation. The Stucky group's contributions have focused on silica and titania as viable scaffolds to treat internal hemorrhage, while the Liu group has focused on dendrimer-, polystyrene- and gold nanoparticles as scaffolds. In coordination with the Morrissey group, research has focused on attaching polyP to all of these scaffolds. Work with the Ismagilov group has focused on determining the threshold conditions for solid silica nanoparticles.

In the coming year, the Ismagilov group will continue to investigate the use of numerical simulations to refine the parameters for TSP-induced blood clotting and identify threshold conditions. They will also obtain approval for drawing blood from human volunteers in order to perform microfluidic tests of the properties of candidate particles using freshly isolated human blood. The Liu group will pursue the most promising candidate polyP-nanoparticles, including gold-, polystyrene- and dendrimer-based particles. The Stucky group hopes to refine the syntheses and capping procedures to provide large quantities potential TSPs to the Ismagilov and Morrissey groups for threshold testing. TSPs will be formed from porous and solid nanoparticles with a low-size dispersion optimized for cardiovascular use and functionalized for an appropriate coagulation agent delivery. Using the primary amine terminus of APTES, procedures are being developed to attach proteins to the nanoparticle scaffolds. Initial TEG reports suggest that the polyP-bound silica nanoparticles accelerate clotting in the presence of recalcified PNP. Biocompatibility studies conducted in collaboration with Dr. Daniele Zink of ASTAR indicate pure silica MCF-26 shows decreased cytotoxicity levels when compared with commonly used coagulating agents such as the aluminosilicate kaolinite. Biocompatibility on other promising materials will continue to ensure that any potential TSP system will not cause harm to the human body. The goal is to identify several new TSP systems with the potential to treat internal hemorrhage.

"So-What Section": The final goal of these studies is to develop advanced nanoparticles engineered to stop internal (incompressible) hemorrhage. If we are successful, we will create regulated clotting activators that can circulate in the blood at below the threshold necessary to trigger clotting, and therefore not cause unwanted thrombosis. However, the nanoparticles will ultimately be engineered to accumulate at sites of internal injury/bleeding, where their local concentration will greatly exceed the threshold for clotting activation, thereby restoring hemostasis. This has the potential to treat otherwise untreatable, life-threatening internal bleeding associated with trauma.

REFERENCES

- [1] Smith SA, Choi SH, Davis-Harrison R, Huyck J, Boettcher J, Reinstra CM, et al. Polyphosphate exerts differential effects on blood clotting, depending on polymer size. *Blood*. 2010;116:4353-9.
- [2] Choi SH, Smith SA, Morrissey JH. Polyphosphate is a cofactor for the activation of factor XI by thrombin. *Blood*. 2011;118:6963-70.
- [3] Smith SA, Mutch NJ, Baskar D, Rohloff P, Docampo R, Morrissey JH. Polyphosphate modulates blood coagulation and fibrinolysis. *Proc Natl Acad Sci U S A*. 2006;103:903-8.
- [4] Smith SA, Morrissey JH. Polyphosphate as a general procoagulant agent. *J Thromb Haemost*. 2008;6:1750-6.
- [5] Smith SA, Morrissey JH. Polyphosphate enhances fibrin clot structure. *Blood*. 2008;112:2810-6.
- [6] Muller F, Mutch NJ, Schenk WA, Smith SA, Esterl L, Spronk HM, et al. Platelet polyphosphates are proinflammatory and procoagulant mediators in vivo. *Cell*. 2009;139:1143-56.
- [7] Wang QZ, Chen XG, Li ZX, Wang S, Liu CS, Meng XH, et al. Preparation and blood coagulation evaluation of chitosan microspheres. *Journal of Materials Science-Materials in Medicine*. 2008;19:1371-7.
- [8] Chen G, Ni N, Zhou J, Chuang Y-J, Wang B, Pan Z, et al. Fibrinogen Clot Induced by Gold-Nanoparticle In Vitro. *Journal of Nanoscience and Nanotechnology*. 2011;11:74-81.
- [9] Kim D, El-Shall H, Dennis D, Morey T. Interaction of PLGA nanoparticles with human blood constituents. *Colloid Surf B-Biointerfaces*. 2005;40:83-91.
- [10] Choi SH, Collins JN, Smith SA, Davis-Harrison RL, Rienstra CM, Morrissey JH. Phosphoramidate end labeling of inorganic polyphosphates: facile manipulation of polyphosphate for investigating and modulating its biological activities. *Biochemistry*. 2010;49:9935-41.
- [11] Agbasi-Porter C, Ryman-Rasmussen J, Franzen S, Feldheim D. Transcription inhibition using oligonucleotide-modified gold nanoparticles. *Bioconjugate Chemistry*. 2006;17:1178-83.
- [12] Liu J-X, Yang D-Z, Shi F, Cai Y-J. Sol-gel deposited TiO₂ film on NiTi surgical alloy for biocompatibility improvement. *Thin Solid Films*. 2003;429:225-30.
- [13] Harmison CR, Landaburu RH, Seegers WH. Some physicochemical properties of bovine thrombin. *J Biol Chem*. 1961;236:1693-6.
- [14] Baker SE, Sawvel AM, Fan J, Shi Q, Strandwitz N, Stucky GD. Blood clot initiation by mesocellular foams: dependence on nanopore size and enzyme immobilization. *Langmuir : the ACS journal of surfaces and colloids*. 2008;24:14254-60.
- [15] Xie H, Smith JW. Fabrication of PLGA nanoparticles with a fluidic nanoprecipitation system. *Journal of nanobiotechnology*. 2010;8:18.
- [16] Schmidt-Winkel P, Lukens JWW, Zhao D, Yang P, Chmelka BF, Stucky GD. Mesocellular siliceous foams with uniformly sized cells and windows. *JACS*. 1999;121:254-5.
- [17] Schmidt-Winkel P, Yang P, Margolese DI, Chmelka BF, Stucky GD. Fluoride-induced hierarchical ordering of mesoporous silica in aqueous acid syntheses. *Advanced Materials*. 1999;11:303-7.
- [18] Zhang Y, Jiang T, Zhang Q, Wang S. Inclusion of telmisartan in mesocellular foam nanoparticles: drug loading and release property. *Eur J Pharm Biopharm*. 2010;76:17-23.
- [19] Margolis J. The effect of colloidal silica on blood coagulation. *The Australian journal of experimental biology and medical science*. 1961;39:249-58.
- [20] Roy SC, Paulose M, Grimes CA. The effect of TiO₂ nanotubes in the enhancement of blood clotting for the control of hemorrhage. *Biomaterials*. 2007;28:4667-72.
- [21] Huang D, Luo GS, Wang YJ. Using phosphoric acid as a catalyst to control the structures of mesoporous titanium dioxide materials. *Microporous Mesoporous Mater*. 2005;84:27-33.
- [22] Lorenz B, Marme S, Muller WE, Unger K, Schroder HC. Preparation and use of polyphosphate-modified zirconia for purification of nucleic acids and proteins. *Anal Biochem*. 1994;216:118-26.
- [23] Morrissey JH, Pureza V, Davis-Harrison RL, Sligar SG, Ohkubo YZ, Tajkhorshid E. Blood clotting reactions on nanoscale phospholipid bilayers. *Thromb Res*. 2008;122 Suppl 1:S23-6.

[24] Neeves KB, Illing DA, Diamond SL. Thrombin flux and wall shear rate regulate fibrin fiber deposition state during polymerization under flow. *Biophys J.* 2010;98:1344-52.

APPENDIX/SUPPORTING DATA

Mesocellular Foam

The items below include nitrogen adsorption/desorption isotherms and pore size distribution for all three mesocellular foams. Figure A-3 shows the x-ray diffraction pattern and Figure A-4 shows the scanning electron microscopy images for MCF-24. Finally, a table lists the properties for all three mesocellular foams.

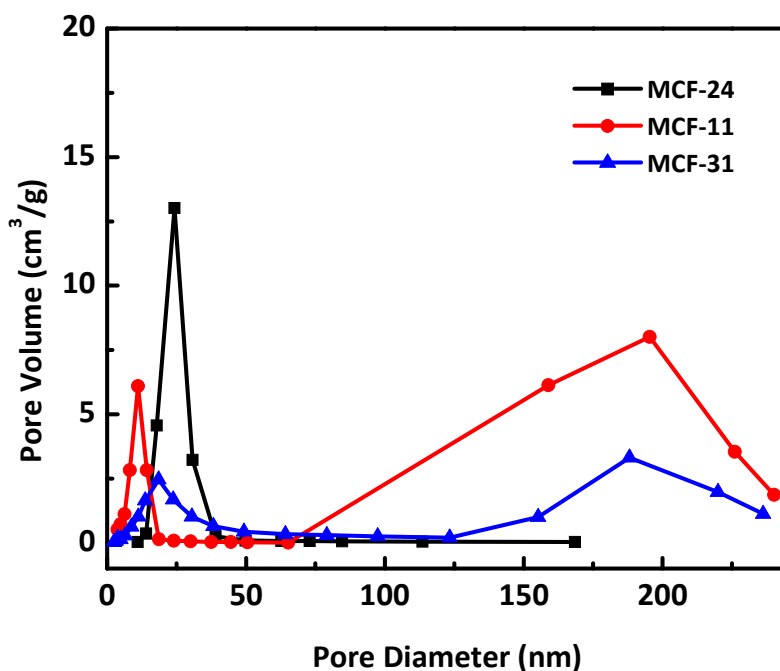


Figure A-1. Pore size distribution of mesocellular foams calculated desorption branch by BJH method.

Table 1 – Textual properties of synthesized mesocellular foams

MCF Sample	BJH Window Size (nm)	BJH Cell Size (nm)	BET Surface Area (m ² /g)	Pore Volume (cm ³ /g)
MCF-11	11.2	19.3	591.7	1.7
MCF-24	24.3	39.3	321.0	2.4
MCF-31	30.9	42.4	222.4	1.6

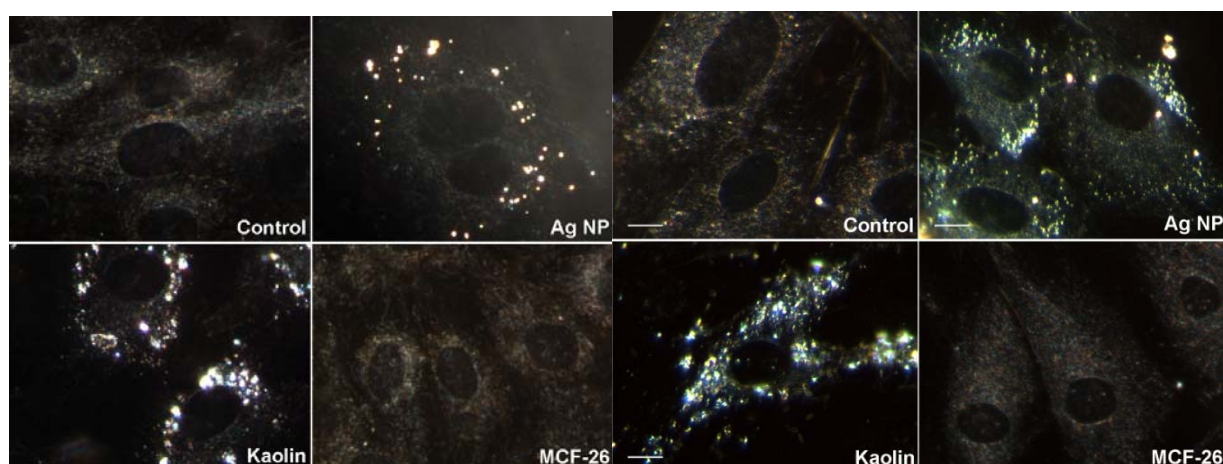


Figure A-2. (Left) Uptake of various samples by HUVEC (Human Umbilical Vein Endothelial Cells). Ag NP concentration – 10 µg/ml; Kaolin concentration - 10 µg/ml; MCF-26 concentration 100 µg/ml. (Right) Uptake of various samples by HDFs. Ag NP concentration – 20 µg/ml; Kaolin concentration - 20 µg/ml; MCF-26 concentration 100 µg/ml.

Table 2 - Neural red uptake assay values for MCF-26.

Cell Type	IC50 (mg / ml)	% Viability at $C_{max} = 7$ mg / ml
HUVEC 5117	6.3 +/- 0.2	50% +/- 3.4 %
HUVEC 5025	2.1 +/- 0.8	26.6 % +/- 6.7 %
HUVEC 3516	0.7 +/- 0.0	20.8 % +/- 2.0
HDF-a (ScienCell)	2.0 +/- 0.2	13.4 % +/- 2.8 %
HDF-a (PromoCell)	5.6 +/- 1.4	39.5 % +/- 8.0 %
HDF-a (ATCC)	5.0 +/- 0.7	41.4 % +/- 3.1 %
HEK-a 6940	> 7.0	91.9 +/- 8.6 %
HEK-a 6937	> 7.0	59.8 % +/- 4.4 %
HEK-a 6539	> 7.0	77.5 % +/- 3.1 %

FMS NPs

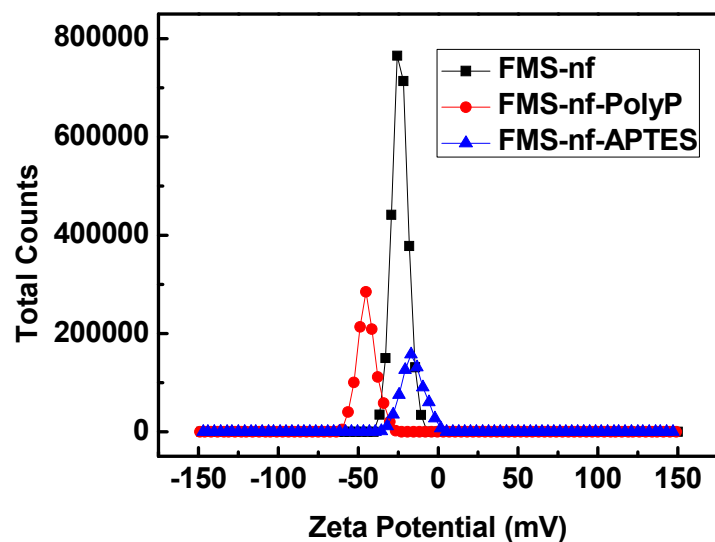


Figure A-3. Zeta potentials of FMS-nf, FMS-nf loaded with polyP, and FMS-nf loaded with APTES particles.

Table 3 – TEG measurements for controlled pooled normal plasma, FMS-ns, and polyphosphate-modified FMS-ns.

Run	R(min)	K(min)	Angle(deg)	MA(mm)
Control Average	13.40	3.70	55.63	37.77
Control St. Dev.	1.28	0.36	7.75	8.35
FMS-ns Average	7.98	1.98	63.93	31.25
FMS-ns St. Dev.	0.67	0.95	12.19	6.43
FMS-ns-PolyP Average	7.03	1.30	77.63	28.43
FMS-ns-PolyP St. Dev.	0.50	0.46	3.52	2.32

PLGA Methodology

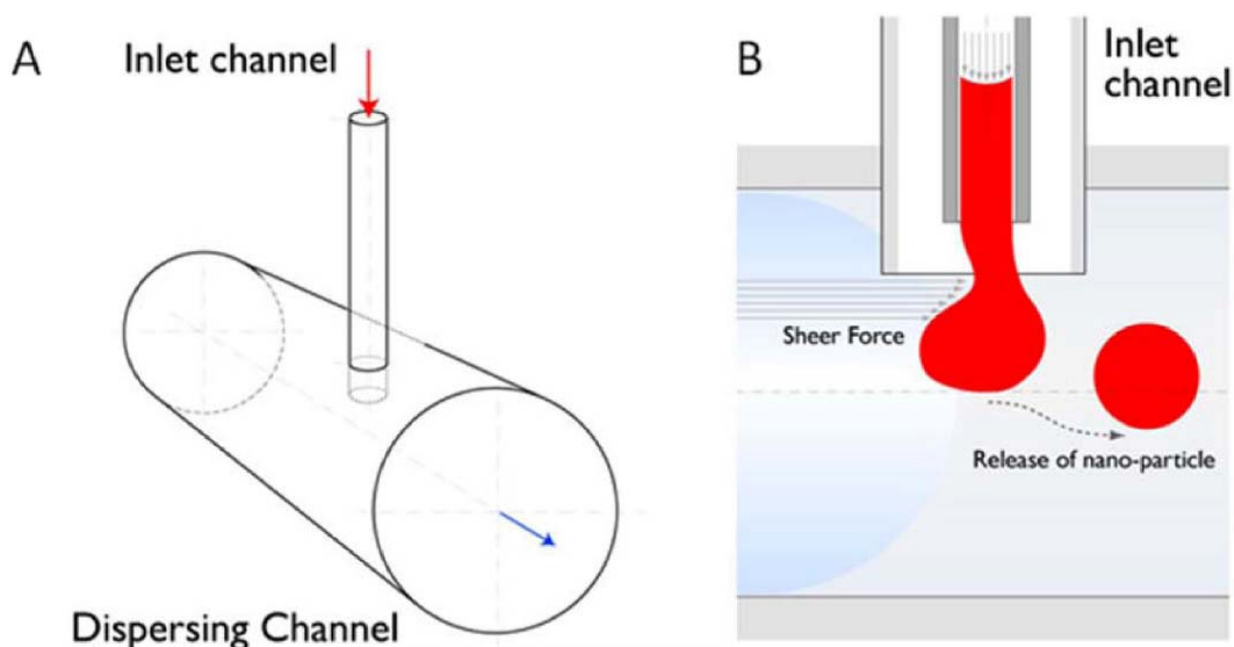


Figure A-4. Schematic of the PLGA-based silica nanoparticle synthesis. (A) Samples are inserted into the dispersing channel. The inlet channel contains sol-gel silica, which precipitates upon contact with the media to form spherical nanoparticles. (B) Side view of the schematic, which illustrates how the spherical nanoparticles form. Particle sizes for PLGA have been demonstrated to average roughly 125 nm [15].

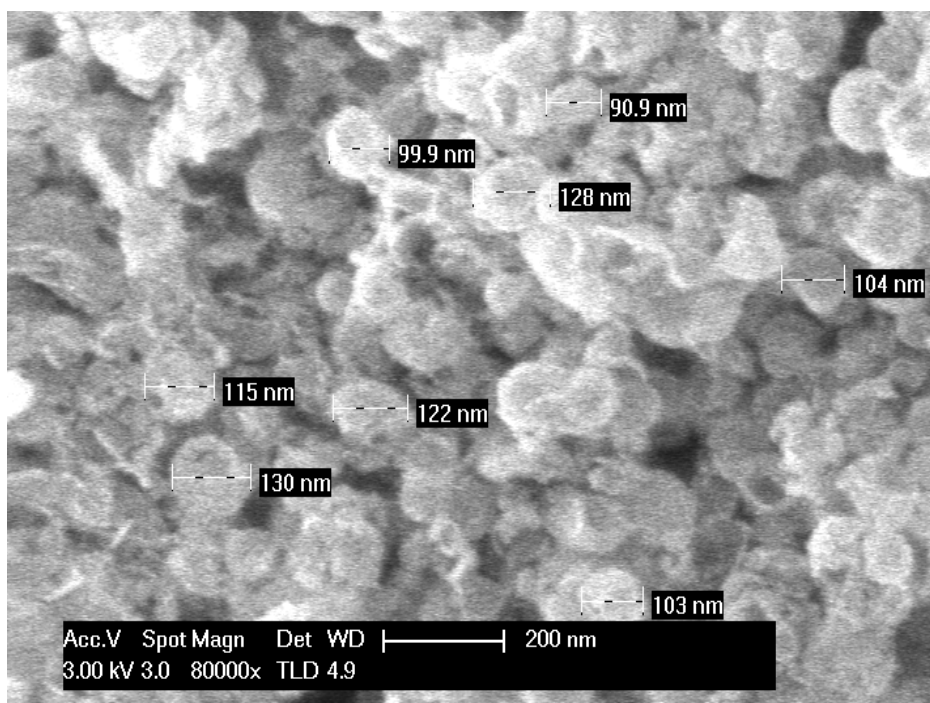


Figure A-5. SEM images of silica NPs prepared using the PLGA system in Figure 5. Average particle diameter 125 +/- 25 nm determined by dynamic light scattering. The conjoined nature of the separate particles occurred due to sputtering for SEM imaging.

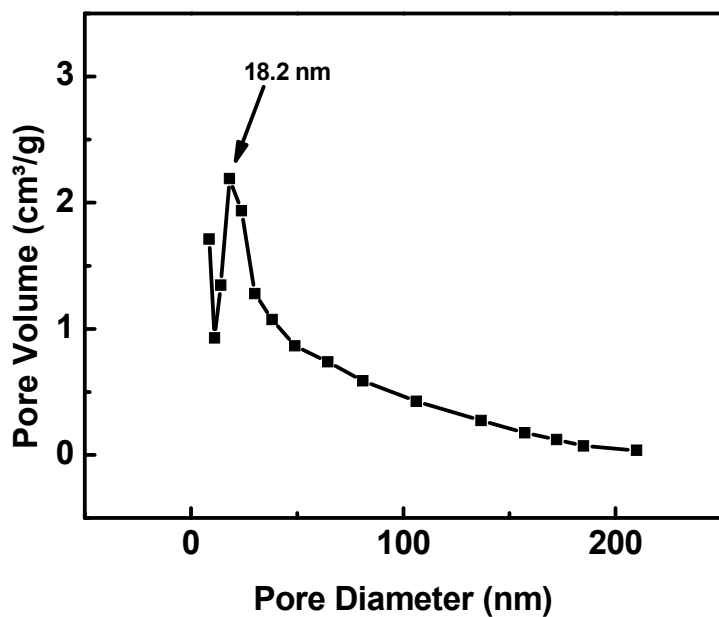


Figure A-6. Pore size distribution of porous silica calculated desorption branch by BJH method.

Titania

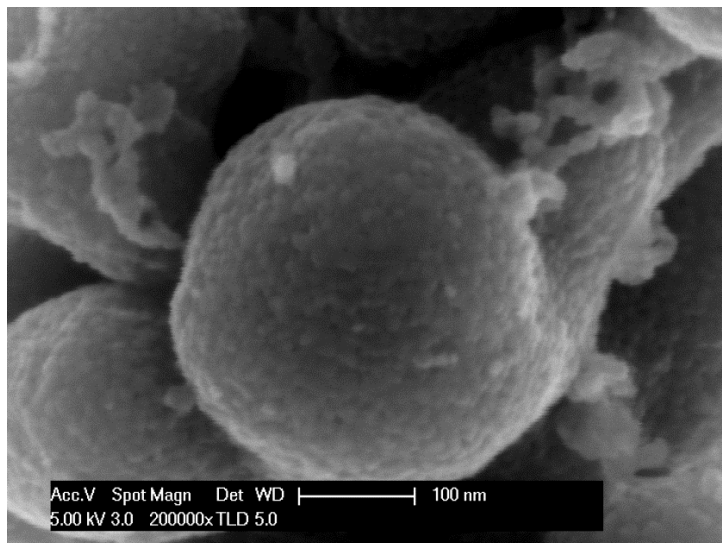


Figure A-7. SEM images of TiO₂ synthesized via the phosphoric acid pathway. The conjoined nature of the separate particles occurred due to sputtering for SEM imaging.

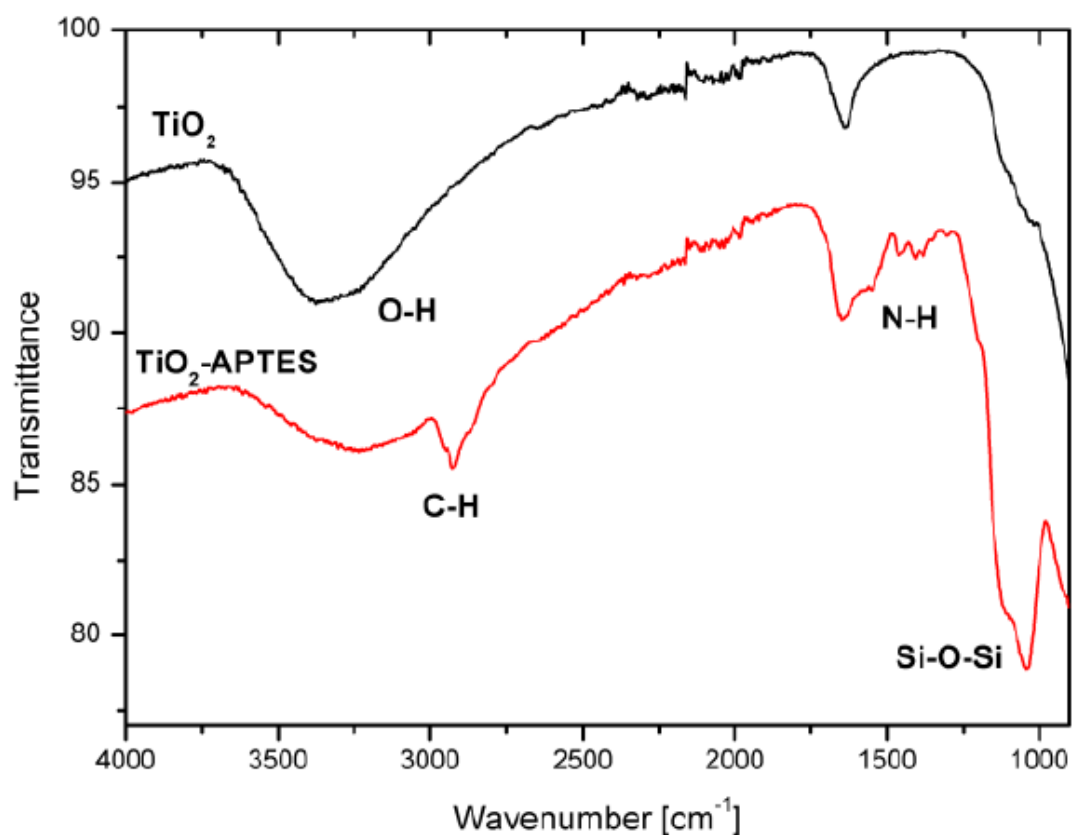


Figure A-8. FT-IR spectrum of unmodified and APTES-modified titania nanoparticles. C-H, N-H, and Si-O-Si bands indicate successful attachment of APTES to TiO₂ molecules.

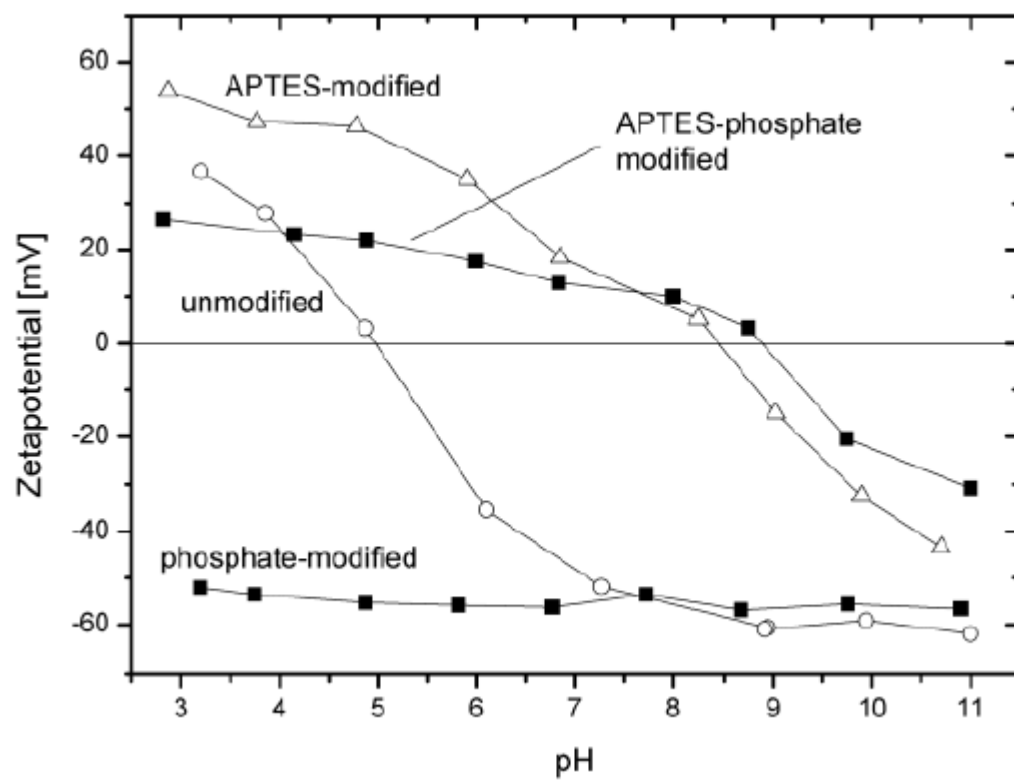


Figure A-9. Zeta potential titration of unmodified and modified titania nanoparticles.